International Journal of Thermophysics, Vol. 19, No. 3, 1998

Effective Thermal Conductivity in a Radial-Flow Packed-Bed Reactor[1]

J. Fuentes,[2] F. Pironti,[2] and A. L. López de Ramos[2,3]

In this work a theoretical and experimental study of the heat transfer process in a radial flow reactor was carried out under steady- and non-steady-state conditions in order to determine the effective thermal conductivity (k_e). One of the mathematical models proposed was a pseudohomogeneous model in which the effective thermal conductivity varies with radial position. The second model studied was a two-phase model with different thermal conductivities for gas and solid. For the pseudohomogeneous model, an analytical solution was obtained using the method of separation of variables and series approximation. In the two-phase model, the gas and solid temperature profiles were obtained by two numerical methods: orthogonal collocation and Runge–Kutta. Several experiments were performed by changing particle diameter, gas flow and temperature input, and reactor size and time-operation condition: steady and nonsteady. Theoretical results were compared with experimental data in order to calculate the effective thermal conductivity. The values of k_e agree in general with the literature data. At low Reynolds numbers there is no appreciable difference between a pseudohomogeneous model and a two-phase equation model. Constant thermal properties can be used at $Re < 5$ with enough accuracy to predict the thermal behavior of a radial-flow reactor.

KEY WORDS: effective thermal conductivity; packed bed; pseudohomogeneous model; radial flow.

1. INTRODUCTION

Radial-flow packed-bed reactors are used in certain processes where high space velocities are required [1]. A complete study of the heat transfer

---

[1] Paper presented at the Thirteenth Symposium on Thermophysical Properties, June 22–27, 1997, Boulder, Colorado, U.S.A.

[2] Grupo de Fenómenos de Transporte, Departmento de Termodinámica y Fenómenos de Transferencia, Universidad Simón Bolívar, Apartado Postal 89.000, Caracas 1080-A, Venezuela.

[3] To whom correspondence should be addressed.

through the packed bed of such reactors is important for a better understanding and a more efficient design of these units. A precise knowledge of the effective thermal properties (i.e., effective thermal conductivity, k_e) is necessary in order to perform a stability phenomena analysis in the case of fixed-bed exothermal reactors.

Several authors have been working in this area. For example, Hlavácek and Votruba [2] recommended the use of data measured in tubular reactors for radial flow adopting a logarithmic average radius. Kunii and Smith [3], Swift [4], Kobayashi [5], Godbee and Ziegler [6], Kuzay [7], Bauer and Schünder [8], Jaguaribe and Beasley [9], and Nozad et al. [10, 11] recommended different methods for the evaluation of the stagnant effective thermal conductivity (k_e^0: effective thermal conductivity at zero velocity). Yagi et al. [12], Kunii and Smith [13], Votruba et al. [14], Gunn and De Souza [15], and Dixon and Cresswell [16] calculated the effective thermal conductivity in axial-flow packed-bed reactors using a steady-state model. Additionally, Juang and Weng [17], Levec and Carbonell [18], and Dixon and Creswell [19] worked with axial-flow packed-bed reactors, but under transient conditions. Finally, Votruba and Hlavácek [20], Pulve et al. [21], López de Ramos and Pironti [22], and Fuentes et al. [23] studied the heat transfer process in radial-flow packed-bed reactors using stationary (the first two) and transient models (the last two references).

The objective of this work was to calculate the effective thermal conductivity using steady state and transient models, assuming that k_e depends on the radial position.

2. EXPERIMENTAL METHODS

The flow diagram of the equipment used (Fig. 1) consists of a radial-flow reactor placed inside a heat insulated cylinder, a set of valves controlling the cold and hot air entrances to the reactor, and an automatic data processing system connected to the reactor thermocouple to register temperature changes in the packed bed. The reactor is composed of two coaxial cylinders of different diameters constructed of stainless-steel sieves, fixed by means of two disks with concentric grooves cut in them, with dimensions corresponding to the major and minor circumferences of the reactor cylinders. A distributing tube, perforated with small, uniformly spread orifices, is placed along the cylindrical axis to ensure correct radial flow of air through the packed bed. An electric tubular resistance is placed inside the distributing tube if the reactor works under steady-state conditions. Temperatures were measured and registered in radial, angular, and

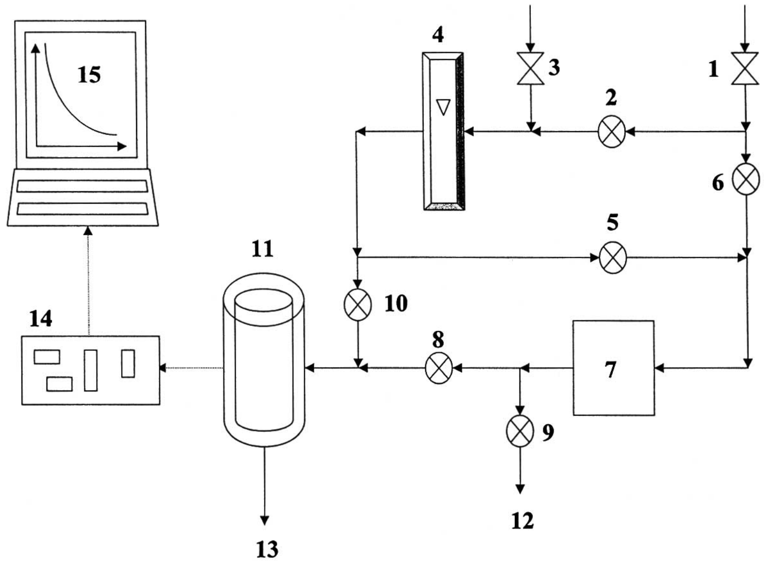

Fig. 1. Experimental setup. 1, 3: Gate valves. 2, 5, 6, 8, 9, 10: Ball valves. 4: Rotameter. 7: Electrical heater system. 11: Reactor vessel. 12, 13: Drains. 14: Data acquisition system. 15: Personal computer.

axial positions (16 ports total). T-type thermocouples (copper–constantant) are placed in a small guide tube, sealing the edge with cement. The packing material consisted of nonreacting polymer and ceramic particles with average diameters between 2×10^{-3} and 5×10^{-3} m. The maximum temperature of the warm air was limited by the melting point of the polymer; the optimum operation range found experimentally was 50 to 60 °C. The cool air temperature was 23 °C. The bed's axial and angular symmetry was verified for each experiment. In fact, temperatures varied in the worst case by 1.5 °C. In the transient case, the temperature of the air going into the reactor was step-increased. In the steady-state case, the tubular electric resistance was set using a Variac. The air flow range was from 6.23 to 9.91 $m^3 \cdot h^{-1}$.

3. MATHEMATICAL MODEL

3.1. Homogeneous Model

Temperature variations inside the bed are analyzed using a pseudo-homogeneous model that does not make any distinction between solid and fluid temperature. A differential heat balance for this model is expressed by an equation such as

$$\langle \rho Cp \rangle \frac{\partial T}{\partial t} + \rho_f Cp_f u \frac{\partial T}{\partial r} = \left(\frac{\partial k_e}{\partial r} + \frac{k_e}{r} \right) \frac{\partial T}{\partial r} + k_e \frac{\partial^2 T}{\partial r^2} \tag{1}$$

where $\langle \rho Cp \rangle$ is the average heat capacity between solid and fluid, T is the temperature, t is the time, ρ_f is the fluid density, Cp_f is the fluid heat capacity, u is the fluid superficial velocity, r is the radial position, and k_e is the effective thermal conductivity.

Yagi et al. [12] have found experimentally that the effective thermal conductivity for axial flow in tubular reactors varies linearly with fluid velocity according to the following expression:

$$\frac{k_e}{k_f} = \frac{k_e^0}{k_f} + \delta \text{ Pr Re} \tag{2}$$

where k_f is the thermal conductivity of the fluid, k_e^0 is the effective thermal conductivity for a stagnant fluid, δ is a correlation parameter, the Prandtl number is calculated as $\text{Pr} = Cp\mu/k_f$, and Re is the Reynolds number calculated as $\text{Re} = \rho_f u D_p/\mu$.

In Eq. (1) it is assumed that the effective thermal conductivity, k_e, is a function of the radial position through the fluid velocity as stated in Eqs. (2) and (3):

$$\frac{1}{r} \frac{\partial (r \rho_f u)}{\partial r} = 0 \tag{3}$$

Then in a radial-flow reactor, the term ru remains constant, but u and therefore Re are a function of r.

3.1.1. *Steady-State Case*

The differential equation for the steady-state case is given by Eq. (1) without the first term. The boundary conditions applied to this problem were

$$\begin{cases} T = T_1 & \text{at} \quad r = R_1 \\ T = T_2 & \text{at} \quad r = R_2 \end{cases} \tag{4}$$

The solution is

$$\frac{T-T_2}{T_1-T_2}=\theta=\frac{(R_2+\delta\ \mathrm{Pe}^*\ d_p)^{\mathrm{Pe}^*}-(r+\delta\ \mathrm{Pe}^*\ d_p)^{\mathrm{Pe}^*}}{(R_2+\delta\ \mathrm{Pe}^*\ d_p)^{\mathrm{Pe}^*}-(R_1+\delta\ \mathrm{Pe}^*\ d_p)^{\mathrm{Pe}^*}} \tag{5}$$

where Pe* is a modified Peclet number given by $\mathrm{Pe}^*=\rho_f urCp/k_e^0$.

3.1.2. Nonsteady Case

Equation (1) is the differential equation for the nonsteady case. The initial and boundary conditions applied were:

$$\begin{aligned}
&t=0, && T=T_0, && R_1<r<R_2\\
&t>0, && k_e\frac{\partial T}{\partial r}=\rho_f Cp_f u(T-T_1), && r=R_1\\
&t>0, && \frac{\partial T}{\partial r}=0, && r=R_2
\end{aligned} \tag{6}$$

The analytical solution of Eq. (1) with the initial and boundary conditions (6) is

$$\phi(r,\tau)=\frac{T-T_1}{T_0-T_1}=\sum_{i=0}^{\infty}C_i[\phi_i^r(r)]\exp\left(-\frac{\lambda_i^2\tau}{1+H}\right) \tag{7}$$

where

$$\begin{aligned}
&\phi_i^r(r)=\mathrm{C1}_i\sum_{j=0}^{\infty}a_j(\lambda_i)(r+\delta\alpha\ \mathrm{Pe}^*)^j+\mathrm{C2}_i\sum_{j=0}^{\infty}b_j(\lambda_i)(r+\delta\alpha\ \mathrm{Pe}^*)^{j+\mathrm{Pe}^*}\\
&H=\frac{\varepsilon\rho_f Cp_f}{(1-\varepsilon)\rho_s Cp_s}\quad\text{and}\quad\tau=\frac{tk_e^0}{\rho_f Cp_f R_1^2}
\end{aligned} \tag{8}$$

The coefficients a_j and b_j have the form of

$$\begin{aligned}
&a_0=1, && b_0=1\\
&a_1=\frac{\delta\alpha\ \mathrm{Pe}^*\ \lambda^2}{1-\mathrm{Pe}^*}, && b_1=\frac{\delta\alpha\ \mathrm{Pe}^*\ \lambda^2}{1+\mathrm{Pe}^*}\\
&a_j=\frac{\lambda^2(\delta\alpha\ \mathrm{Pe}^*\ a_{j-1}-a_{j-2})}{j(j-\mathrm{Pe}^*)}, && j\geqslant 2,\\
&b_j=\frac{\lambda^2(\delta\alpha\ \mathrm{Pe}^*\ b_{j-1}-b_{j-2})}{j(j+\mathrm{Pe}^*)}, && j\geqslant 2
\end{aligned} \tag{9}$$

The eigenvalues λ_i are calculated as the positive roots of the following equation:

$$U(\lambda_i)\, S(\lambda_i) - W(\lambda_i)\, V(\lambda_i) = 0 \tag{10}$$

where

$$\begin{aligned} U(\lambda_i) &= \sum_{j=0}^{\infty} j a_j(\lambda_i) \left(\frac{R_2}{R_1} + \delta\alpha\, \mathrm{Pe}^*\right)^{j-1}, \\ W(\lambda_i) &= \sum_{j=0}^{\infty} (j + \mathrm{Pe}^*)\, b_j(\lambda_i) \left(\frac{R_2}{R_1} + \delta\alpha\, \mathrm{Pe}^*\right)^{j+\mathrm{Pe}^*} \\ V(\lambda_i) &= \sum_{j=0}^{\infty} (j - \mathrm{Pe}^*)\, a_j(\lambda_i)(1 + \delta\alpha\, \mathrm{Pe}^*)^j, \\ S(\lambda_i) &= \sum_{j=0}^{\infty} j b_j(\lambda_i)(1 + \delta\alpha\, \mathrm{Pe}^*)^{j+\mathrm{Pe}^*} \end{aligned} \tag{11}$$

The constants $\mathrm{C1}_i$ and $\mathrm{C2}_i$ and C_i can be calculated using the following expressions:

$$\mathrm{C1}_i = -W(\lambda_i), \qquad \mathrm{C2}_i = U(\lambda_i), \qquad \text{and} \qquad \underline{C_i} = \underline{\underline{A_{ij}^{-1}}}\, \underline{B_i} \tag{12}$$

where

$$A_{i,j} = \int_1^{R_2/R_1} \phi_i^r(r)\, \phi_j^r(r)\, dr, \qquad B_i = \int_1^{R_2/R_1} \phi_i^r(r)\, dr \tag{13}$$

3.2. Two-Phase Model

Temperature variations inside the bed can be analyzed using a two-phase model that makes a distinction between solid and fluid temperature. A differential heat balance for this model is expressed by the equations

$$\frac{1}{r}\frac{\partial}{\partial r}\left(r k_{\mathrm{af}} \frac{\partial T_{\mathrm{f}}}{\partial r}\right) - \rho_{\mathrm{f}} Cp_{\mathrm{f}} u \frac{\partial T_{\mathrm{f}}}{\partial r} - ah(T_{\mathrm{f}} - T_{\mathrm{s}}) = \varepsilon \rho_{\mathrm{f}} Cp_{\mathrm{f}} \frac{\partial T_{\mathrm{f}}}{\partial t} \tag{14}$$

$$\frac{1}{r}\frac{\partial}{\partial r}\left(r k_{\mathrm{rs}} \frac{\partial T_{\mathrm{s}}}{\partial r}\right) + ah(T_{\mathrm{f}} - T_{\mathrm{s}}) = (1 - \varepsilon)\, \rho_{\mathrm{s}} Cp_{\mathrm{s}} \frac{\partial T_{\mathrm{s}}}{\partial t} \tag{15}$$

where k_{af} is the axial fluid-phase effective thermal conductivity, k_{rs} is the solid-phase effective thermal conductivity, and h is the fluid-solid heat transfer coefficient.

The initial and boundary conditions for this model are

$$t=0 \rightarrow T_f = T_0, \qquad T_s = T_0 \qquad \text{for all } r \tag{16}$$

$$t>0 \rightarrow \frac{\partial T_f}{\partial r} = 0, \qquad \frac{\partial T_s}{\partial r} = 0 \qquad r = R_2 \tag{17}$$

$$t>0 \rightarrow k_{af}\frac{\partial T_{af}}{\partial r} = \rho_f C p_f u (T_f - T_1), \qquad T_s = T_f \qquad r = R_1 \tag{18}$$

The correlation reported by Zehner and Schlünder [24] was used to calculate the solid-phase effective thermal conductivity, k_{rs}. This conductivity is assumed constant with position:

$$\frac{k_{rs}}{k_f} = \sqrt{1-\varepsilon}\,\frac{k_{rs}^0}{k_f} \tag{19}$$

To calculate the fluid-phase effective thermal conductivity, k_{af}, the correlation proposed by Edwards and Richardson [25] was used. In this case, k_{af} is a function of the position through the fluid velocity:

$$\frac{1}{\mathrm{Pe}_{af}} = \frac{k_{af}}{\rho_f u D_p C p_f} = \frac{0.73\varepsilon}{\mathrm{Re\,Pr}} + \frac{0.5}{1 + (9.7\varepsilon)/(\mathrm{Re\,Pr})} \tag{20}$$

The fluid-solid heat transfer coefficient, h, was calculated by Stuke's correlation [26] that assumed h as a function of the Reynolds number.

An analytical solution for this coupled system of nonlinear partial differential equations may be difficult to find, so an orthogonal collocation method (with 11 collocation points) was chosen combined with a Runge–Kutta method in order to obtain the corresponding temperature profiles.

4. RESULTS AND DISCUSSION

Figure 2 shows a typical temperature response for the nonsteady case after the temperature of the air was step-increased from $T_0 = 23\,°\mathrm{C}$ to $T_1 = 66\,°\mathrm{C}$. The top line corresponds to the gas entrance temperature, close to a perfect step temperature input. Initially the bed responds slowly to the change of temperature, and after 3 h, the temperature inside the reactor was almost uniform and constant. For this reason, it was necessary to introduce an electric heater inside the reactor to study its thermal behavior under steady-state conditions.

Figure 3 shows three radial temperature profiles for the steady-state case. The radial reactor used has a R_2/R_1 ratio equal to 6, a particle

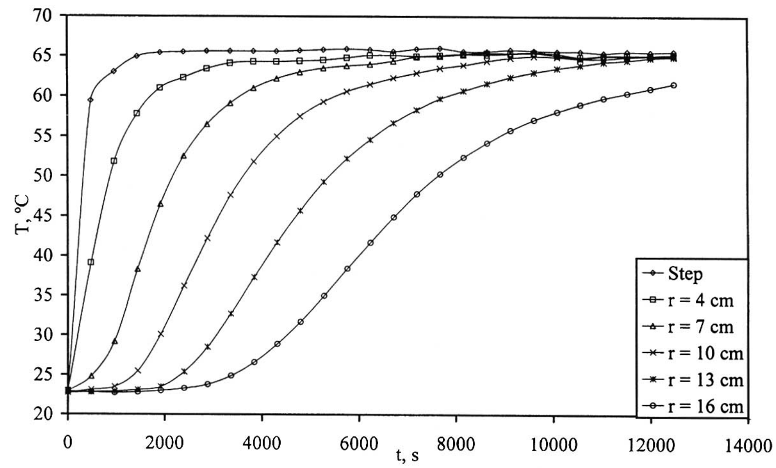

Fig. 2. Temperature response for the nonsteady case after a temperature air step from $T_0 = 23\,°C$ to $T_1 = 66\,°C$. Ratio $R_2/R_1 = 4$; particle diameter = 4.2 mm; gas input flow = 19.51 $m^3 \cdot h^{-1}$.

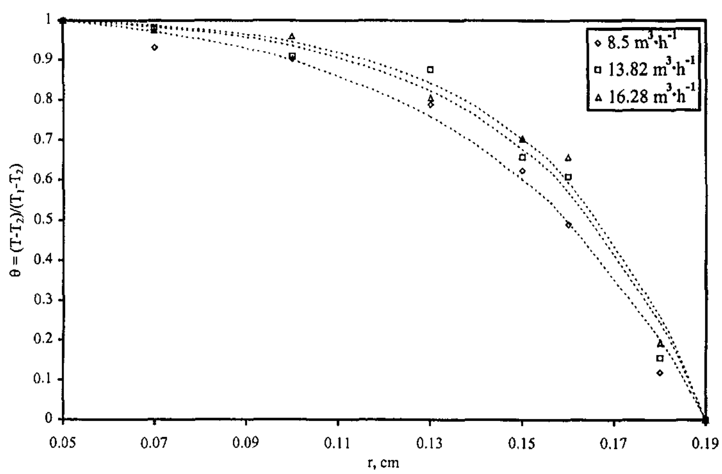

Fig. 3. Radial temperature profile for the steady-state case. Ratio $R_2/R_1 = 6$; particle diameter = 3.3 mm; gas input flows = 8.5, 13.8, and 16.3 $m^3 \cdot h^{-1}$.

diameter of 3.3 mm, and gas input flows of 8.5, 13.8 and 16.3 $m^3 \cdot h^{-1}$. The dotted lines represent the theoretical values obtained using Eq. (4). The value of δ adjusted for all steady-state experiments was 5. An acceptable agreement between experimental and theoretical values is observed. This behavior was found in all the experiments performed under different operating conditions.

Figure 4 contains all the k_e values calculated in this work for the steady state. For all the steady-state cases, the value of δ that best fit the temperature profile is 5 (in the range of Reynolds numbers studied). This value is one order of magnitude higher than the value reported by Yagi et al. [12] for axial flow in tubular reactors. As expected, the variation of k_e as a function of RePr was linear [Eq. (2)].

Figure 5 shows the Peclet number values as a function of the Reynolds number including others experimental results reported previously, indicating good agreement. It can be observed that non-steady-state experimental values are similar to those calculated under steady-state conditions. This behavior agrees with the result obtained by Dixon and Cresswell [19] for the axial flow reactors at small Reynolds numbers. Then the effective parameter (k_e) can be considered the same for steady-state and transient models for the radial-flow packed-bed reactors at Reynolds numbers less than 5.

The temperature response for a reactor with a ratio R_2/R_1 equal to 6 for $Pe^* = 714$ is shown in Fig. 6. The dimensionless temperatures were calculated using Eq. (6) and the numerical solution of Eqs. (9) and (13).

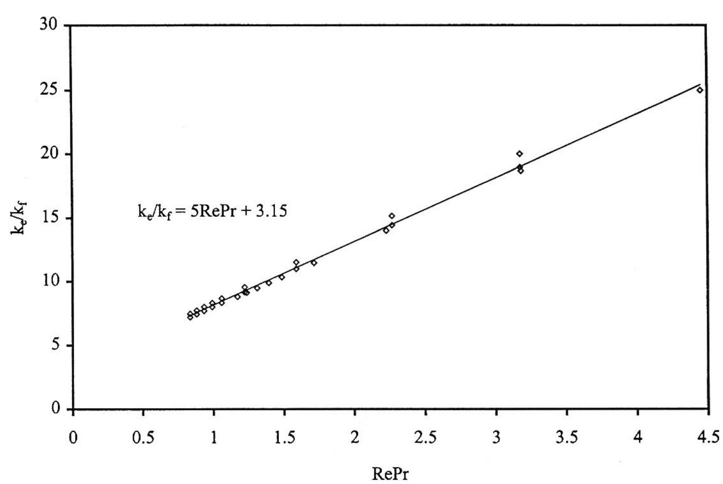

Fig. 4. k_e as a function of RePr using the steady-state model.

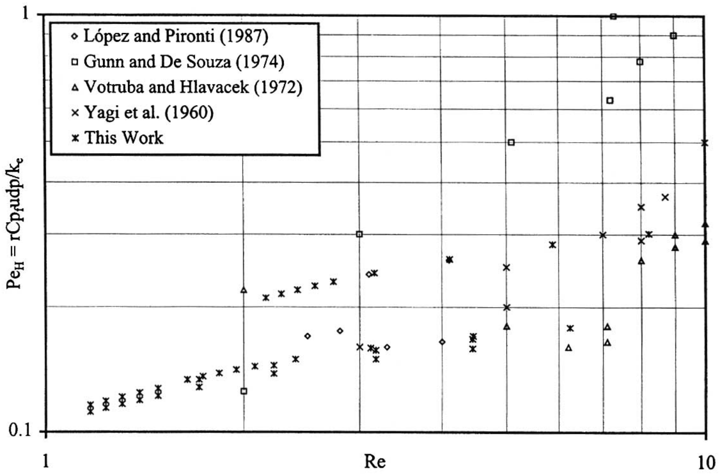

Fig. 5. Pe_H as a function of Re for the steady-state and transient models.

There is an acceptable concordance between the pseudohomogeneous and the two-phase models for low Reynolds numbers. The pseudohomogeneous temperature profile is located between the solutions for solid- and gas-phase profiles. However, for high Reynolds numbers, a large difference is observed between the corresponding profiles, indicating disagreement between the two models. A pseudo-homogeneous equation can be used

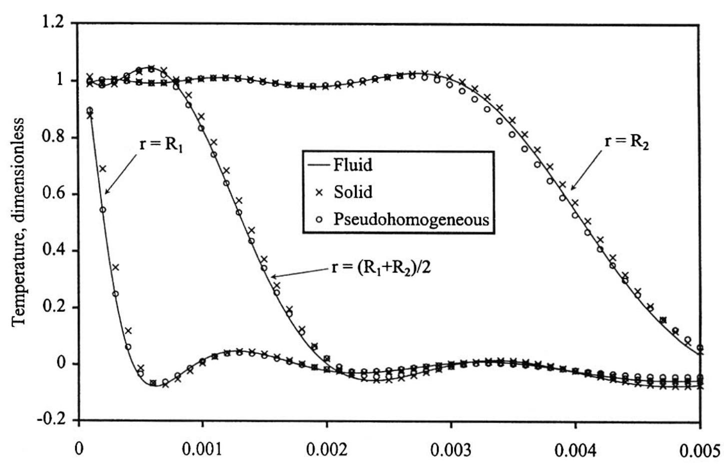

Fig. 6. Temperature response for $Pe^* = 714$, $R_2/R_1 = 6$, and particle diameter = 4.2 mm for a nonsteady method.

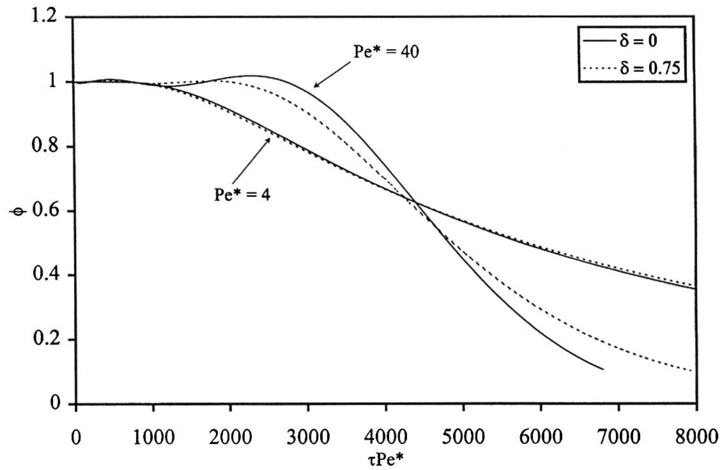

Fig. 7. Influence of δ values in temperature responses.

instead of the two-phase equations for low Reynolds numbers, but it is not recommended for high Reynolds numbers.

Figure 7 shows a case where the effective thermal conductivity can be approximated by a constant along the reactor bed for radial flow. In this case the dimensionless temperature is almost the same when δ goes from 0 to 0.75 for low modified Peclet number (around 4). Nevertheless, for a Pe* equal to 40 the difference between taking k_e constant and variable is significant. Then it is possible to simplify the model to one with k_e constant at low Reynolds (Pe*) numbers and use the analytical solution found by López de Ramos and Pironti [22].

5. CONCLUSIONS

For the pseudohomogeneous model, an analytical solution was obtained using the method of separation of variables and a series approximation. In the two-phase model, the gas and solid temperature profiles were obtained by two numerical methods: orthogonal collocation and Runge–Kutta. Theoretical results were compared with experimental data in order to calculate the effective thermal conductivity. The values of k_e agree in general with the literature data.

At low Reynolds numbers there is no appreciable difference between a pseudohomogeneous model and a two-phase equation model. Constant thermal properties can be used at $Re < 5$ with enough accuracy to predict the thermal behavior of a radial-flow reactor. Furthermore, there was no difference between steady-state and transient methods for experimental determination of the effective thermal conductivity at low Reynolds numbers. At high Reynolds numbers it is recommended that a two-phase model with a variable fluid-phase effective thermal conductivity is used.

ACKNOWLEDGMENTS

The authors want to thank the *Decanato de Investigaciones y Desarrollo* of the *Universidad Simón Bolivar* and *CONICIT* (Project No. S1-95-000476) for their financial support.

REFERENCES

1. V. Vek, *Ind. Eng. Chem. Process Des. Dev.* **16**:412 (1977).
2. V. Hlávacek and J. Votruba, in *Chemical Reactor Theory. A Review*, De L. Lapidus and N. Amundson, eds. (Prentice Hall, Englewood Cliffs, NJ, 1977).
3. D. Kunii and J. M. Smith, *AIChE J.* **6**:71 (1960).
4. D. L. Swift, *Int. J. Heat Mass Transfer* **9**:1061 (1966).
5. M. Kobayashi, in *Handbook of Heat Transfer Applications*, De. W. M. Rohsenow, J. P. Hartnett, and E. J. Ganic, eds. (McGraw-Hill, New York, 1985).
6. H. W. Godbee and W. T. Ziegler, in *Handbook of Heat Transfer Applications*, De W. M. Rohsenow, J. P. Hartnett, and E. J. Ganic, eds. (McGraw-Hill, New York, 1985).
7. T. M. Kuzay, in *Handbook of Heat Transfer Applications*, De W. M. Rohsenow, J. P. Hartnett, and E. J. Ganic, eds. (McGraw-Hill, New York, 1985).
8. R. Bauer and E. V. Schkünder, *Ind. Chem. Eng.* **18**:189 (1978).
9. E. F. Jaguaribe and D. E. Beasley, *Int. J. Heat Mass Transfer* **27**:399 (1984).
10. Y. Nozad, R. G. Carbonell, and S. Whitaker, *Chem. Eng. Sci.* **40**:843 (1985).
11. Y. Nozad, R. G. Carbonell, and S. Whitaker, *Chem. Eng. Sci.* **40**:857 (1985).
12. S. Yagi, D. Kunii, and N. Wakao, *AIChE J.* **6**:543 (1960).
13. D. Kunii and J. M. Smith, *AIChE J.* **7**:29 (1961).
14. J. Votruba, V. Hlavácek, and M. Marek, *Chem. Eng. Sci.* **27**:1845 (1972).
15. D. J. Gunn and J. F. C. De Souza, *Chem. Eng. Sci.* **29**:1363 (1974).
16. A. G. Dixon and D. L. Cresswell, *AIChE J.* **25**:663 (1979).
17. H. D. Juang and H. S. Weng, *Int. J. Heat Mass Transfer* **26**:1275 (1983).
18. J. Levec and R. G. Carbonell, *AIChE J.* **31**:581 (1985); **31**:591 (1985).
19. A. G. Dixon and D. L. Cresswell, *AIChE J.* **32**:809 (1986).
20. J. Votruba and V. Hlavácek, *Chem. Eng. J.* **9**:91 (1972).
21. I. Pulve, A. L. López de Ramos, and F. Pironti, in *V Congreso Latinoamericano de Transferencia de Calor y Materia, Tomo I* (1994) IIC-3.1–IIC-3.11.
22. A. L. López de Ramos and F. Pironti, *AIChE J.* **33**:1747 (1987).
23. J. Fuentes, A. López de Ramos, and F. Pironti, in *Memorias del IV Simposio Latinoamericano sobre Propiedades de Fluidos y Equilibrio de Fases para el Diseño de Procesos Químicos: EQUIFASE'95, EQ-34*, (1995), pp. 1–10.
24. P. Zehner and E. P. Schünder, *Chem.-Ing. Technik* **42**:933 (1970).
25. M. F. Edwards and J. F. Richardson, *Chem. Eng. Sci.* **23**:109 (1968).
26. B. Stuke, *Angewandte Chem.* **B20**:262 (1948).